A&A 390, 369–381 (2002)
DOI: 10.1051/0004-6361:20020729

Astronomy & Astrophysics

D/HD transition in Photon Dominated Regions (PDR)

F. Le Petit, E. Roueff, and J. Le Bourlot

LUTH and FRE2462 du CNRS, Observatoire de Paris, Place J. Janssen, 92195 Meudon Cedex, France
e-mail: Franck.Lepetit@obspm.fr,Jacques.lebourlot@obspm.fr

Received 10 July 2001 / Accepted 15 May 2002

Abstract. We present the basic features of a steady state chemical model of Photon Dominated Regions (PDR), where the deuterium chemistry is explicitly introduced. The model is an extension of a previous PDR model (Abgrall et al. 1992; Le Bourlot et al. 1993; Le Bourlot 2000) in which the microscopic processes relative to HD have been incorporated. The J-dependent photodissociation probabilities have been calculated and included in the statistical equilibrium of the rotational levels of HD where the latest collision molecular data are also introduced. The thermal balance is calculated from the equilibrium between the different heating and cooling processes. We introduce a standard model of density $n_{\rm H} = 500$ cm^{-3} embedded in the Interstellar Standard Radiation Field (ISRF) from which we derive the main properties of HD in PDR. The D/HD transition does not depend only on the density, radiation field but also on the chemical processes and especially on the dust formation efficiency. In standard radiation field conditions, the D/HD transition occurs in a narrow range of visual extinctions as long as density is less than 1000 cm^{-3} and HD is formed through the $D^+ + H_2$ reaction. At higher densities a logarithmic dependence of the location of the transition is derived. The model is applied both to ultraviolet absorption observations from the ground rotational state of HD performed in diffuse and translucent clouds and infrared emission detectable at high densities and for high ultraviolet radiation fields coming from the bright surrounding stars.

Key words. astrochemistry – molecular processes – ISM: molecules

1. Introduction

Since deuterium has been formed only at the early beginning of the universe, the elemental deuterium to hydrogen ratio is one pivotal parameter to understand the evolution of astrophysical media. In the interstellar medium (ISM), deuterium may be present in atomic but also in molecular form and over 20 single D-bearing molecules and two doubly deuterated ones have been found in cold molecular clouds and star forming regions (Roueff et al. 2000; Loinard et al. 2000). Last but not least, the triply deuterated ammonia has been detected towards two dense cold clouds (Lis et al. 2002; van der Tak et al. 2002). However, chemical fractionation processes and mantle desorption from grains take place in these molecular clouds and it is not straightforward to derive the elemental deuterium abundance from such observations (Roberts & Millar 2000a,b).

Atomic deuterium has first been observed with the Copernicus satellite in the local interstellar medium and in diffuse clouds in absorption towards bright stars where HD has also been detected (see Lemoine et al. 1999 for a review). The successful launch of the FUSE (Far Ultraviolet Spectroscopy Explorer) mission allows to search for molecular HD towards fainter sources, in translucent clouds which are intermediate between diffuse and molecular clouds. FUSE detections of interstellar HD have been reported in a variety of galactic lines of sight (Ferlet et al. 2000; Rachford et al. 2001; Lacour et al. 2002; Boissé et al. 2002) and in the LMC (Bluhm & De Boer 2002). Moreover, the short wavelength spectrograph (SWS) of the ISO (Infrared Space Observatory) satellite has allowed the observations of the pure rotational emission transitions of HD at 112 μm (J = 1–0) (Wright et al. 1999) in the Orion Bar and at 19.43 μm (J = 6–5) (Bertoldi et al. 1999) in Orion KL. Finally, the 2.64 μm, (1–0) R(5) line of HD has also been detected in Orion Peak 1 by Ramsay Howat et al. (2002) at UKIRT. These two last detections have been performed in shocked regions where the present paper does not apply.

From the modelling point of view, Black & Dalgarno (1973) have first considered the atomic to molecular transition of deuterium in diffuse clouds to interpret Copernicus observations. Viala et al. (1988a) have developed a more elaborate model of diffuse clouds in the same context where the photochemical equilibrium is solved at a fixed temperature. Meanwhile, the rotational and rovibrational collisional excitation of HD by H, He and H_2 has been studied with quantal close coupling techniques and new molecular potential surfaces (Roueff & Zeippen 1999, 2000; Flower & Roueff 1999). Transition and photodissociation probabilities of H_2 and HD have been improved (Abgrall et al. 2000; Abgrall & Roueff 2002) taking into account the rotational coupling and new transition moments calculations.

Send offprint requests to: E. Roueff,
e-mail: Evelyne.Roueff@obspm.fr

We present in this paper an updated PDR model where the chemistry as well as the microscopic processes of HD have been introduced. The chemical and statistical equilibrium are solved together with the thermal balance and the most recent molecular data have been included. The basic features of the model are discussed in Sect. 2. In Sect. 3, a standard model is presented and the influence of the various physical parameters (density, intensity of the incident radiation field, rate of formation of HD on dust) is considered. Comparison with observations are reviewed in Sect. 4.

2. PDR model

2.1. General features

The present study is a straightforward extension of the steady state PDR model of Abgrall et al. (1992), Le Bourlot et al. (1993) and Le Bourlot (2000). We consider a steady state model of an interstellar cloud as an infinite slab of gas and dust irradiated by an ultraviolet radiation field impinging on one side of the cloud. The incoming ultraviolet radiation field is expressed in units of the ISRF model of Draine (1978). The radiative transfer is solved in decoupling the continuum extinction due to dust and gas and the absorption in lines of H_2, HD and CO. In addition, we use the approximation introduced by Federman et al. (1979) to estimate the self-absorption in the dissociating lines of H_2, HD and CO, and we neglect the overlap between the lines of H_2 and other molecules. This approximation reproduces the main physical properties as shown by Abgrall et al. (1992) and allows rapid computations.

The abundances of 139 chemical species linked by a network of 1416 chemical reactions are computed as a function of the visual extinction. These species consist of H, D, He, O, C, N, S and a representative metal M. The elemental depletions are taken from the recent HST observations and the gas phase abundances are displayed in Table 1. Since the elemental abundance of deuterium is not well known, it can be considered as a free parameter with a value close to 1.6×10^{-5} (Linsky et al. 1995), the mean value in the local ISM. In the present model, we have arbitrarily fixed it at 2×10^{-5}.

The chemical equations are solved in parallel to the excitation processes (see next section) and include J-dependent photodissociation rates of H_2, HD and CO.

Thermal balance is solved as discussed in Le Bourlot et al. (1993). The heating due to photoelectric effect on grains has been updated following Le Bourlot (2000) where the actual magnitude of the ISRF is calculated at the different visual extinctions. The charge of the grains and the resulting photoelectric heating are functions of the grain size, following the derivation of Bakes & Tielens (1994). Cooling processes are principally due to radiative emission following excitation of abundant atoms and molecules. We derive the level populations of the various coolants (C, C^+, O, H_2, HD, CO, CS, HCO^+) by solving the corresponding statistical equilibrium. Then we compute the local emissivities corresponding to the cooling emission, taking into account possible optical depths effects.

Table 1. Elemental gas phase abundances.

D/H[1]	2×10^{-5}
O/H[2]	3.19×10^{-4}
He/H	1×10^{-1}
N/H[3]	7.5×10^{-5}
C/H[4]	1.32×10^{-4}
S/H[4]	1.85×10^{-6}
M/H	1.5×10^{-8}

[1] free parameter in our model.
[2] Meyer et al. (1998).
[3] Meyer et al. (1997).
[4] Savage et Sembach (1996).

At the edge of the cloud, all atoms with ionization energies smaller than 13.6 eV, the ionization threshold of atomic hydrogen, are mainly ionic and the others are predominantly neutral. Formation of H_2 takes place on grains in competition with destruction by photodissociation. The medium becomes progressively molecular as the visual extinction increases and photodissociation probability decreases, (van Dishoeck & Black 1986; Abgrall et al. 1992). The H/H_2 and the C^+/C/CO transitions in the envelopes of interstellar clouds have been the subject of many modelling studies (van Dishoeck & Black 1988; Viala et al. 1988b; Hollenbach & Tielens 1999), including those undertaken in our own group (Le Bourlot et al. 1993). There have been much less studies on the D/HD transition (Black & Dalgarno 1973; Viala et al. 1988b), regarding to the very few observational data available up to now.

The H_2 molecule and its deuterated substitute, HD, present very similar properties. The photodissociation mechanisms resulting from fluorescence towards the continuum of the ground electronic state following discrete absorption transitions in the Lyman and Werner band systems are identical. However, the substitution of a proton by a deuteron, leads to some significant differences with H_2. First, HD possesses a small permanent dipole moment of 8.3×10^{-4} Debye due to the shift between the center of mass and the center of charge. So electric dipole transitions, whose probabilities have been calculated by Abgrall et al. (1982), occur between rovibrational levels within the ground state, whereas only electric quadrupole transitions are possible for H_2. Secondly, the chemical formation processes of HD and H_2 are different as discussed in Sect. 2.3.

The parameters of the models are the proton density $n_{\rm H}$ (in $\rm cm^{-3}$), the cosmic ray ionization rate of H_2, ζ (in $\rm s^{-1}$), the Doppler turbulent parameter b (in km $\rm s^{-1}$) and the scaling factor χ of the ISRF in Draine's unit. The grain properties play a considerable role, both for the chemistry (formation of H_2 and HD) and for the thermal balance. In the actual model, we take the standard galactic values of the mass per unit volume, the albedo and asymmetry factor of the grains (g) as well as the dust to gas mass ratio (G). We introduce the size distribution of the grains as a power law with exponent 3.5 following Mathis et al. (1977) and an analytic dependence of the extinction curve from the UV to the visible using the Fitzpatrick & Massa (1990) expansion coefficients. The corresponding values

Table 2. Standard values of the grain parameters.

albedo	0.42
g	0.6
ρ (g/cm^{-3})	3
G	0.01
$r_{\rm min}$ (μm)	0.003
$r_{\rm max}$ (μm)	0.3
N_H/A_V (1)	1.87×10^{21}
$c1$	−0.38
$c2$	0.74
$c3$	3.96
$c4$	0.26
γ	1.05
λ_0^{-1}	4.59

(1) from Bohlin et al. (1978) expressed in cm^{-2} mag $^{-1}$.
Values in the second part of the chart are the coefficients of the galactic extinction curve parameterized by Fitzpatrick & Massa (1990).

as well as the relation between the total proton column density and the visual extinction are given in Table 2.

2.2. Excitation of HD

We solve the statistical equilibrium of the nine first rotational levels of HD, with energy terms below the first excited vibrational level. The corresponding energies are given in Table 3.

We consider three possible contributions to the excitation: radiative pumping, collisions and chemical formation. Radiative pumping involves absorption by the electronic Lyman and Werner transitions. The excited B and C electronic states decay towards the discrete rovibrational levels of the ground state or towards the continuum, which leads to dissociation of the HD molecule (occurs in approximately 15% of cases). The excited rovibrational levels of the ground electronic state cascade towards the rotational ground state via faint electric dipole transitions with $|\Delta J| = 1$ selection rule as calculated by Abgrall et al. (1982). Collisional excitations occur with the most abundant species in the cloud: H, He, H_2 and electrons. Finally, the chemical formation processes of HD may also contribute to its excitation. We apply the cascade formalism introduced first by Black & Dalgarno (1976) for molecular hydrogen and extended to HD and C_2 respectively by Viala et al. (1988b) and Le Bourlot et al. (1987). We assume that the rovibrational levels of the ground electronic state with energies higher than 4 445 K (corresponding to the level $v = 0$, $J = 8$) are only decaying via spontaneous radiative transitions. Then, the equations governing the time evolution of the abundances of the nine first rotational levels of HD, n_{0J}, can be written:

$$\frac{{\rm d}n_{0J}}{{\rm d}t} = \left(\frac{{\rm d}n_{0J}}{{\rm d}t}\right)_{\rm rad.} + \left(\frac{{\rm d}n_{0J}}{{\rm d}t}\right)_{\rm coll.} + \left(\frac{{\rm d}n_{0J}}{{\rm d}t}\right)_{\rm chemistry}. \quad (1)$$

Table 3. Energies of the first levels of HD.

Level	Energy in Kelvin
$v = 0$ $J = 0$	0.
$v = 0$ $J = 1$	128.38
$v = 0$ $J = 2$	384.26
$v = 0$ $J = 3$	765.89
$v = 0$ $J = 4$	1270.7
$v = 0$ $J = 5$	1895.4
$v = 0$ $J = 6$	2635.9
$v = 0$ $J = 7$	3487.5
$v = 0$ $J = 8$	4445.3
$v = 1$ $J = 0$	5226.7

The equation describing the excitation by radiative processes can be written as:

$$\left(\frac{{\rm d}n_{0J}}{{\rm d}t}\right)_{\rm rad.} = d_{0J} + D_{0J} - n_{0J} \sum_{J'<J} A_{0J,0J'} - n_{0J} \sum_{B,C} \sum_{v'J'} B_{0J,v'J'} \int_{912}^{\infty} u(\lambda) \cdot \phi_{0J,v'J'}(\lambda)\, {\rm d}\lambda \quad (2)$$

where $u(\lambda)$ is the density of the energy of the interstellar ultraviolet radiation field and $\phi_{0J,v'J'}$ is the profile of the line for the considered transition. B and C refer to the excited electronic states, and $v'J'$ labels a rovibrational level belonging to one of these excited electronic states. d_{0J} is the summation of the direct radiative de-excitation terms from the electronic excited levels $v'J'$ toward level $0J$ of the ground electronic state and D_{0J} is the total de-excitation term due to the radiative cascades inside the ground electronic state:

$$d_{0J} = \sum_{B,C} \sum_{v'j'} A_{v'J',0J} n_{v'J'}$$
$$D_{0J} = \sum_{v''J''} A_{v''J'',0J}\, n_{v''J''}. \quad (3)$$

Levels $v''J''$ and $0J$ belong to the ground electronic state with $E(v''J'') > E(0J)$.

The contribution of collisions to the rotational populations of HD is:

$$\left(\frac{{\rm d}n_{0J}}{{\rm d}t}\right)_{\rm coll.} = \sum_q \sum_{J''=0}^{J=8} K^q_{0J'',0J} n_{J''} n_q - \sum_q \sum_{J''=0}^{J=8} K^q_{0J,0J''} n_{0J} n_q. \quad (4)$$

In this equation, $K^q_{0J'',0J}$ is the collision rate of HD with a perturber q for the transition from the level $0J''$ toward the level $0J$. In the present case, we consider as possible perturbers, electrons, H, He and H_2.

Finally, the contribution of chemistry to the excitation of HD gives:

$$\left(\frac{{\rm d}n_{0J}}{{\rm d}t}\right)_{\rm chemistry} = \sum_m k_m n_X n_Y p^m_{0j} - \sum_l k_l n_Z n_{0J} \quad (5)$$

where n_X, n_Y and n_Z are the densities of the reagents, k_m is the rate coefficient of the m chemical reaction and p^m_{0J} is the probability to produce HD in the level $0J$ through this reaction.

The various contributions are calculated with the most recent molecular data. Previous transition probabilities in the Lyman and Werner band systems have been calculated by Allison & Dalgarno (1970) in a single state approximation and assuming that $J = 0$. We introduce the values calculated by Abgrall & Roueff (2002) where the rotational coupling and centrifugal barrier potential are taken into account in the resolution of the Schrödinger equation. The rovibrational collisional excitation and de-excitation rate coefficients of H_2 and HD by H, He and H_2, are those reported in Flower et al. (2000). They are expressed as analytical functions of the temperature and can be found at url: `http://ccp7.dur.ac.uk`.

The critical density (the minimum density required to reach thermodynamical equilibrium in a two-level approximation) is the ratio between the Einstein spontaneous de-excitation rate and the collisional de-excitation rate coefficient:

$$n_{\rm crit}(J) = \frac{A_{J,J-1}}{K_{J,J-1}}.$$

In this equation, $K_{J,J-1}$, is the weighted sum of the collisional de-excitation rate coefficients of all the perturbers:

$$K_{J,J-1} = \sum_q \frac{n(q)}{n} K^q_{J,J-1}$$

where n is the value of the actual density.

We have computed the critical densities of levels $J = 1$ to $J = 8$ of HD in function of the temperature, both for an atomic gas and a molecular gas. Results are presented in Tables 4 and 5. We note that the values are typically larger than 1000 cm^{-3} for $J = 1$ and that they decrease with temperature, reflecting the temperature dependence of the collisional rate coefficients. Critical density values increase significantly with J. Chemical excitation seems unlikely to compete with collisional or radiative processes.

Table 4. Critical densities $n_{\rm crit}$ in cm^{-3} of HD levels in a neutral gas mixture of H and He with a fractional abundance of He equals to 0.1.

Level	T = 10 K	50 K	100 K	200 K	500 K
$J = 1$	6.1×10^3	4.5×10^3	3.3×10^3	2.0×10^3	9.4×10^2
$J = 2$	5.8×10^4	4.1×10^4	2.9×10^4	1.7×10^4	7.1×10^3
$J = 3$	2.3×10^5	1.6×10^5	1.1×10^5	6.3×10^4	2.5×10^4
$J = 4$	7.4×10^5	5.0×10^5	3.3×10^5	1.8×10^5	6.8×10^4
$J = 5$	3.7×10^6	2.1×10^6	1.2×10^6	5.2×10^5	1.5×10^5
$J = 6$	7.9×10^6	4.5×10^6	2.6×10^6	1.1×10^6	3.0×10^5
$J = 7$	1.5×10^7	8.8×10^6	5.0×10^6	2.2×10^6	5.7×10^5
$J = 8$	2.1×10^7	1.3×10^7	8.2×10^6	3.8×10^6	1.0×10^6

Table 5. Critical densities $n_{\rm crit}$ in cm^{-3} of HD levels in a neutral gas mixture of H_2 and He with the number density ratio of He to H_2 of 0.2. Ortho and para populations of H_2 have been taken at the thermal equilibrium.

Level	T = 10 K	50 K	100 K	200 K	500 K
$J = 1$	3.3×10^3	2.6×10^3	2.0×10^3	1.4×10^3	8.0×10^2
$J = 2$	2.0×10^4	1.7×10^4	1.4×10^4	1.0×10^4	5.7×10^3
$J = 3$	9.1×10^4	7.2×10^4	5.6×10^4	3.9×10^4	2.0×10^4
$J = 4$	3.6×10^5	2.8×10^5	2.0×10^5	1.2×10^5	5.5×10^4
$J = 5$	8.1×10^5	6.2×10^5	5.1×10^5	3.4×10^5	1.4×10^5
$J = 6$	5.9×10^6	3.6×10^6	2.1×10^6	9.4×10^5	2.8×10^5
$J = 7$	1.3×10^7	8.7×10^6	5.1×10^6	2.3×10^6	6.1×10^5
$J = 8$	3.6×10^7	2.2×10^7	1.3×10^7	5.3×10^6	1.2×10^7

2.3. Chemistry of HD

The gas phase chemistry of HD has been discussed in the context of primordial clouds by Galli & Palla (1998) and Stancil et al. (1998). We have introduced the corresponding reactions in the present model, in addition to the previous updated network that has been used in the context of shock chemistry (Pineau des Forêts et al. 1989).

Whereas H_2 formation occurs only on dust, the formation of HD may involve surface as well as gas phase processes. Formation on dust is assumed to occur similarly to H_2. A first step involves the adsorption of D and H at the surface of the grains. The two adsorbed atoms meet then on this surface and gaseous HD is desorbed. We note D: and H: respectively the adsorbed deuterium and adsorbed hydrogen.

$$\begin{cases} \mathrm{D} + \mathrm{dust} \xrightarrow{k_{\rm ads}} \mathrm{D}: & k_{\rm ads} = s < n_{\rm gr}\sigma > v \quad (\mathrm{s}^{-1}) \\ \mathrm{H} + \mathrm{dust} \xrightarrow{k'_{\rm ads}} \mathrm{H}: & k'_{\rm ads} = s' < n_{\rm gr}\sigma > v' \quad (\mathrm{s}^{-1}) \\ \mathrm{D}: + \mathrm{H}: \xrightarrow{k_{\rm dust}} \mathrm{HD} \end{cases} \tag{6}$$

In these equations, the adsorption rate coefficient $k_{\rm ads}$ can be expressed as the product of the sticking coefficient, s, the relative velocity of the atom to the grain, v, and the average over the size distribution of the grains of the product of the geometric cross section of the grains, σ, by the density of grains $n_{\rm gr}$. The sticking coefficient s is a decreasing function of temperature (Hollenbach & Mc Kee 1979). We assume here that the sticking coefficient equals 1 when T is smaller than 10 K and varies as $T^{-1/2}$ at larger temperatures. The adsorption rate coefficient becomes then independent on the temperature for values larger than 10 K since the atomic velocity is proportional to $\sqrt{T}$. The formation rate of H_2 and HD on grains (respectively $\mathcal{FR}(H_2)$ and $\mathcal{FR}$(HD)) can be expressed respectively as:

$$\begin{aligned} \left.\frac{{\rm d}n(\mathrm{H_2})}{{\rm d}t}\right|_{\rm dust\ form.} &= \frac{1}{2}k'_{\rm ads}n(\mathrm{H}) = \mathcal{FR}(\mathrm{H_2})n(\mathrm{H}) \\ \left.\frac{{\rm d}n(\mathrm{HD})}{{\rm d}t}\right|_{\rm dust\ form.} &= k_{\rm ads}n(\mathrm{D}) = \mathcal{FR}(\mathrm{HD})n(\mathrm{D}). \end{aligned} \tag{7}$$

Following Le Bourlot et al. (1995) and Roueff (2002), $k_{\rm ads}$ can be expressed by:

$$k_{\rm ads} = s \cdot \frac{3}{4} \cdot 1.4 \cdot m_{\rm H} \frac{G}{\rho} \frac{1}{\sqrt{r_{\rm max} \cdot r_{\rm min}}}\, v\, n_{\rm H} \tag{8}$$

with $m_{\rm H}$ the mass of the atom of hydrogen and $n_{\rm H}$ the density of protons. Using the parameters in Table 2, we obtain:

$$\begin{aligned} \mathcal{FR}(H_2) &= 4.4 \times 10^{-17} \times n_{\rm H} \quad (\mathrm{s}^{-1}) \\ \mathcal{FR}(HD) &= 6.3 \times 10^{-17} \times n_{\rm H} \quad (\mathrm{s}^{-1}). \end{aligned}$$

These values are very close to the first derivation of the formation rate of H_2 by Jura (1975) from Copernicus observations in diffuse clouds and to the one deduced by Gry et al. (2002) from FUSE observations.

As soon as H_2 is present, gas phase chemical processes may contribute efficiently to the formation of HD. In diffuse clouds, the relevant reaction is:

$$D^+ + H_2 \xrightarrow{k_1} H^+ + HD \qquad k_1 = 2 \times 10^{-9} \ (cm^3\ s^{-1}). \tag{9}$$

The reverse reaction involving an endothermicity of about 464 Kelvin is not efficient in cold regions.

On the other hand, in dense PDRs illuminated by a strong radiation field, the temperature may reach several hundred Kelvin. Then the neutral neutral reaction between D and H_2, may become the most efficient process of formation of HD:

$$D + H_2 \xrightarrow{k_2} H + HD \quad k_2 = 7.5 \times 10^{-11} e^{-3820/T} (cm^3\ s^{-1}). \tag{10}$$

The corresponding chemical formation rates are respectively:

$$\left.\frac{dn(HD)}{dt}\right|_{D^+ + H_2} = k_1 n(D^+) n(H_2) = 2.1 \times 10^{-9} n(D^+) n(H_2) \tag{11}$$

$$\left.\frac{dn(HD)}{dt}\right|_{D + H_2} = k_2 n(D) n(H_2) = 7.5 \times 10^{-11} e^{-3820/T} n(D) n(H_2). \tag{12}$$

It can be shown that the abundance of D^+ is almost independent on the density. Then, the rate of formation of HD through the reaction between D^+ and H_2 is proportional to the density (Eq. (11)). This is no more the case when formation of HD on dust or when the reaction between D and H_2 takes place. The rate of formation of HD is then proportional to the square of the density (Eqs. (7, 12)). We infer that in diffuse clouds, the main route of formation of HD is the reaction in gas phase between D^+ and H_2 as noted previously by Black & Dalgarno (1973). However, formation on dust or formation by the reaction between neutral atomic deuterium and molecular hydrogen becomes competitive and even dominant when the density is larger than about $5{\times}10^3$ cm^{-3}. In such clouds, formation of HD occurs on dust at low temperatures and by the gas phase reaction between D and H_2 for high temperatures. Nevertheless, we should keep in mind that the rate of formation on dust is not well known whereas a relative good agreement between different studies is achieved for the reaction rate coefficient involving D and H_2.

At the edge of the cloud and up to regions where atomic deuterium becomes molecular, destruction of HD occurs mainly by photodissociation. Nevertheless, in the case of a dense and warm molecular cloud, the reaction between HD and H, which is the reverse reaction of Eq. (10), is not negligible:

$$HD + H \xrightarrow{k_2'} H_2 + D \quad k_2' = 7.5 \times 10^{-11} e^{-4240/T} (cm^3\ s^{-1}). \tag{13}$$

Once photo-processes are negligible, destruction by chemical processes becomes dominant. Chemical fractionation of deuterated molecules occurs as reviewed recently by Roberts & Millar (2000a,b) and Le Petit & Roueff (2002). The important step towards other deuterated molecules is the proton transfer reaction of H_3^+ in the reaction with HD forming H_2D^+:

$$H_3^+ + HD \xrightarrow{k} H_2D^+ + H_2 \qquad k = 3.5 \times 10^{-10} \ (cm^3\ s^{-1}). \tag{14}$$

The reverse reaction is endothermic when H_2 is in its ground rotational state $J = 0$ and its efficiency depends on the amount of ortho H_2 present in the environment (Gerlich et al. 2002).

3. Results

3.1. Standard model

We consider a standard chemical model of translucent cloud where the elemental gas phase abundances and dust properties are given in Tables 1 and 2. In addition, we take the following physical parameters: density $n_H = 500$ cm^{-3}, cosmic ray ionization rate $\zeta = 5 \times 10^{-17}$ s^{-1}, turbulent velocity $b = 2$ km s^{-1} and an incident radiation field corresponding to the ISRF ($\chi = 1$).

Figure 1 displays on its upper panel, the photodissociation rates of H_2 and HD as a function of A_V and on its lower panel, the normalized abundances, on one hand, of H and H_2, and on the other hand, of D and HD as a function of A_V. The photodissociation rates (in s^{-1}) of H_2 and HD are the same when $A_V = 0$. This reflects the identity of the microscopic processes. The respective decrease of the photodissociation rates of H_2 and HD is due to the absorption of the radiation field by grains and to the self-shielding. Self-shielding becomes efficient as soon as the optical depths of the discrete absorbing transitions is of the order of 1. The optical depth in the center of the lines of H_2 or HD, $\tau_{H_2/HD}$, is given by:

$$\tau_{H_2/HD} = \frac{\pi e^2}{m_e c} f_{lu} \frac{\lambda_0}{\sqrt{\pi} \cdot \sqrt{v_{turb}^2 + 2kT/m_{H_2/HD}}} \times N_l(H_2/HD) = \frac{1.497 \times 10^{-2} \lambda_0 f_{lu}}{\sqrt{v_{turb}^2 + 2kT/m_{H_2/HD}}} N_l(H_2/HD) \quad (CGS) \tag{15}$$

with f_{lu} the oscillator strength of the Lyman and Werner band systems, λ_0 the wavelength in the center of the line, $N_l(H_2/HD)$, the column density of H_2 or HD in the lower level, m_e the mass of the electron and $m_{H_2/HD}$ the mass of H_2 or HD. As oscillator strengths of the Lyman and Werner band systems are typically of the order of 10^{-3} and the wavelength of the order of 100 nm, the optical depth reaches a value of 1 when the column density of H_2 or HD is about 10^{15} cm^{-2}. As deuterium is typically 10^{-5} times less abundant than hydrogen, self-shielding effects take place at larger visual extinctions; the formation of HD occurs deeper in the cloud than H_2. The comparison of both panels of Fig. 1 shows that the H/H_2 transition and the D/HD one are strongly linked to the photodissociation rates.

Temperature profile, obtained as a result of the thermal equilibrium in the gas phase, is displayed in function of A_V in Fig. 2. Temperature ranges from 70 Kelvin at the edge of the cloud to 10 Kelvin at visual extinctions larger than 2. The H/H_2 transition takes place for $A_V \simeq 3 \times 10^{-3}$ at about 70 Kelvin whereas the D/HD transition occurs at $A_V \simeq 0.5$ where the temperature is close to 50 K.

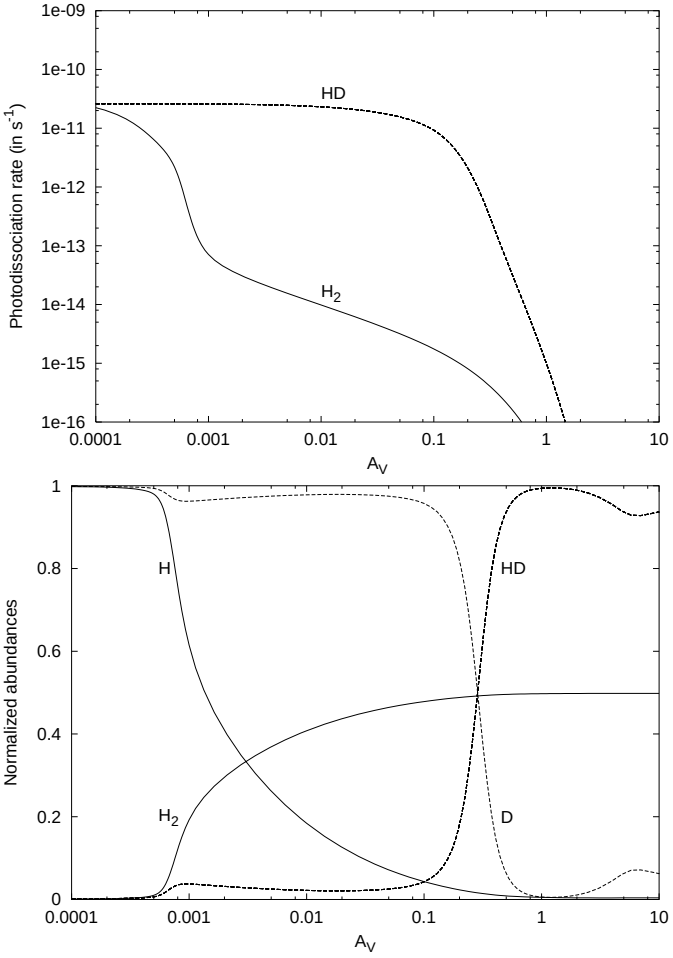

Fig. 1. Transition H/H_2 and D/HD in the standard models. On top panel, photodissociation rates in s^{-1} of H_2 and HD versus A_V. On bottom panel, normalized abundances of H, H_2, D and HD as a function of A_V.

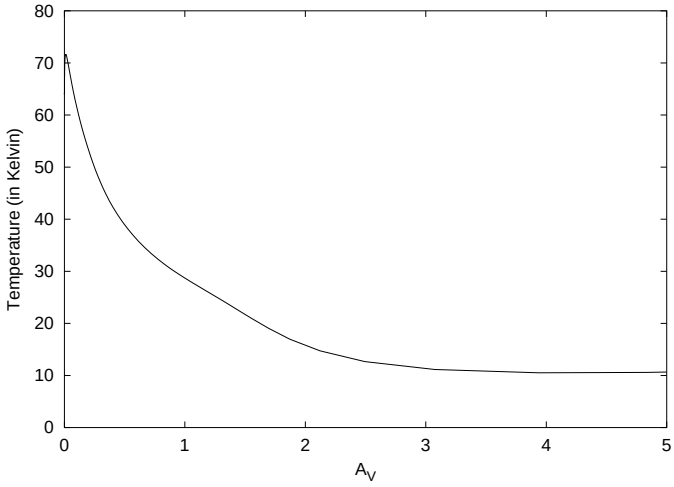

Fig. 2. Profile of the gas temperature as a function of A_V in the standard model.

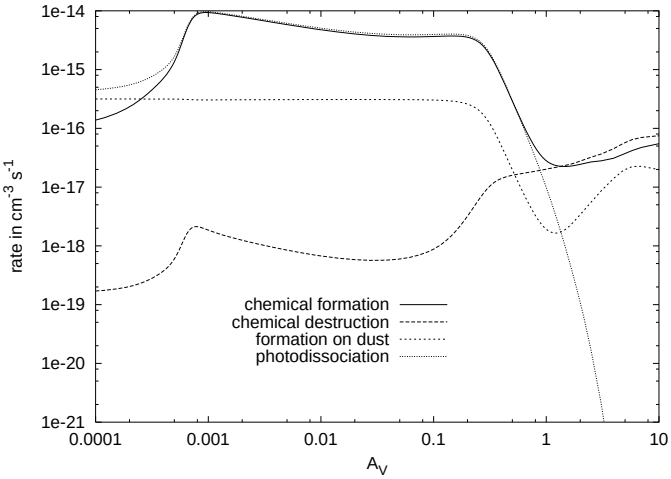

Fig. 3. Formation and destruction rates of HD in cm^{-3} s^{-1} versus visual extinction in the case of the standard model.

The contributions of the different chemical processes related to the formation and the destruction of HD are displayed in Fig. 3. In this model, formation of HD on dust takes place as long as no molecular hydrogen is present. Once H_2 is available, HD is formed through the reaction between D^+ and H_2 (reaction 9). Photodissociation of HD dominates over other chemical destruction processes up to a visual extinction of about 1 magnitude.

There is a significant range of visual extinctions where deuterium is mainly atomic whereas hydrogen is predominantly molecular (cf. Fig. 1). The molecular fraction derived from the observations is defined as:

$$f = \frac{2N(\mathrm{H_2})}{N(\mathrm{H}) + 2N(\mathrm{H_2})} \tag{16}$$

where N(H) and $N(H_2)$ are the atomic and molecular column densities of hydrogen. Figure 4 displays the ratio of the atomic column densities, N(D)/N(H), and of the molecular column densities, N(HD)/$2N(H_2)$, as a function of the molecular fraction for the same standard model. We note that the atomic ratio, N(D)/N(H), is larger than the elemental D/H ratio as soon as HD is present. The corresponding enhancement can reach about one order of magnitude for molecular fractions larger than 0.3. Such a possibility was already pointed out by Black & Dalgarno (1973). On the other hand, the molecular ratio, N(HD)/$2N(H_2)$, is lower than the elemental ratio as long as deuterium is not totally in molecular form contrary to hydrogen. So, the derivation of the elemental value of deuterium from either atomic or molecular observations should be taken with care.

3.1.1. Excitation of HD

We display in Fig. 5 the column densities of the three first rotational levels of HD (J = 0, 1 and 2). The column density of HD J = 0 increases as a function of the visual extinction, whereas those of J = 1 and J = 2 levels become stationary from A_V about 0.5, where the temperature is lower than 40 K (cf. Fig. 2). We find that the corresponding populations are sub-thermal as the density is below the critical density (cf. Tables 4 and 5). The column densities at A_V = 1, are respectively 2.8×10^{16} cm^{-2}, 3.0×10^{14} cm^{-2} and 6.9×10^{10} cm^{-2}, for J = 0, 1 and 2.

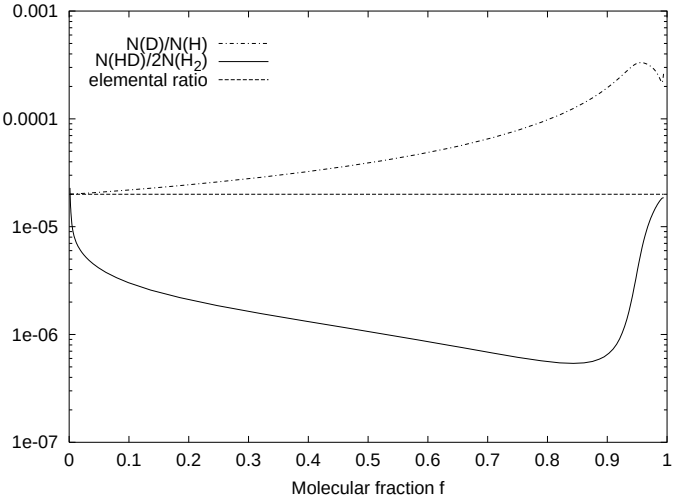

Fig. 4. Ratio of column densities N(D)/N(H) and N(HD)/2N(H_2) as a function of the molecular fraction for the standard model. The horizontal line displays the D/H elemental ratio adopted in the model: 2×10^{-5}.

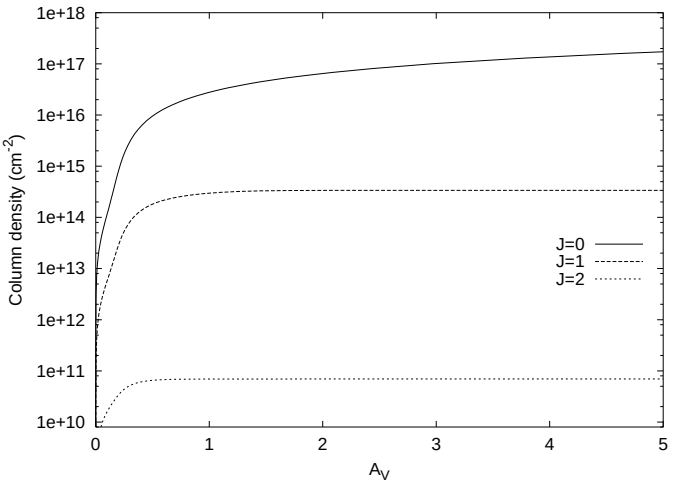

Fig. 5. Column densities of HD in the fundamental and first rotational levels, $J = 0$, $J = 1$ and $J = 2$ in function of A_V in the case of the standard model.

3.2. Dependence on the cloud parameters

3.2.1. Role of the cosmic ray ionization rate

Hartquist et al. (1978) have shown that the cosmic ionization rate could be derived from the observations of OH and HD. Approximate formulae of the steady state abundances of HD and OH have been obtained by Federman et al. (1996), for a molecular fraction of 1/3, i.e. when $n(\mathrm{H})/n(\mathrm{H_2}) \simeq 2$.

The first step of the chemistry of OH and HD involves the cosmic ray ionization of atomic hydrogen:

$$\mathrm{H} + \mathrm{c.r.} \xrightarrow{k_\zeta} \mathrm{H^+} + \mathrm{e^-} \tag{17}$$

where c.r. stands for cosmic ray. This reaction is followed by slightly endothermic charge exchange reactions between H^+ and D (ΔH = 43 K) or O (ΔH = 227 K) producing D^+ and O^+. Then, reactions of D^+ and O^+ with H_2 lead respectively to the formation of HD (Eq. (9)) and to a sequence of reactions leading to the formation of OH. As long as photodissociation dominates the destruction of HD, the steady state abundance of HD can be expressed by:

$$n(\mathrm{HD}) \simeq \frac{k_1\, k_3\, n(\mathrm{H_2})\, n(\mathrm{D})}{\mathcal{P}_\tau(\mathrm{HD})} \times \frac{k_\zeta\, n(\mathrm{H}) + k''_\zeta\, n(\mathrm{H_2}) + k_4\, n(\mathrm{H_2})\, n(\mathrm{H_e^+})}{[k'_3\, n(\mathrm{H}) + k_1\, n(\mathrm{H_2})][k_5\, n(\mathrm{O}) + \alpha(\mathrm{H^+})\, n(\mathrm{e^-})]} \tag{18}$$

with

$$n(\mathrm{H_e^+}) \simeq \frac{k'_\zeta\; n(\mathrm{H_e})}{\alpha(\mathrm{H_e^+})\, n(\mathrm{e^-}) + k_4\, n(\mathrm{H_2})}$$

where $\mathcal{P}_\tau$(HD) is the photodissociation rate (in $\mathrm{s^{-1}}$) of HD at the optical depth τ. The corresponding reaction rate coefficients, k_i, are given in Table 6.

As for OH, its steady state abundance can be written:

$$n(\mathrm{OH}) \simeq \frac{\alpha_2 + \alpha_3}{\alpha_1 + \alpha_2 + \alpha_3}\; \frac{k_5\, n(\mathrm{O})}{\mathcal{P}_\tau(\mathrm{OH}) + k_6\, n(\mathrm{C^+})} \times \frac{k_\zeta\, n(\mathrm{H}) + k''_\zeta\, n(\mathrm{H_2}) + k_4\, n(\mathrm{H_2})\, n(\mathrm{H_e^+})}{k_5\, n(\mathrm{O}) + \alpha(\mathrm{H^+})\, n(\mathrm{e^-})}$$

$$\text{with} \qquad n(\mathrm{C^+}) = \frac{\mathcal{P}_\tau(\mathrm{C})\, n(\mathrm{C})}{\alpha(\mathrm{C^+})\, n(\mathrm{e^-})}. \tag{19}$$

In this equation, $\mathcal{P}_\tau$(C) and $\mathcal{P}_\tau$(OH) are respectively the photoionization rate of carbon and the photodissociation rate of OH at the optical depth τ.

Our expressions differ slightly from those given by Federman et al. (1996). In particular, they remain valid in the range where H is mainly molecular whereas HD is still photodissociated efficiently. This can be seen in Eqs. (18) and (19), where the numerator of the second fraction expresses the production of H^+ not only through cosmic ray ionization of atomic hydrogen (sole case considered by Federman et al.) but also via cosmic ray ionization of molecular hydrogen and via $He^+ + H_2$. So, the abundances of HD and OH are proportional to the cosmic ionization rate, ζ.

Once chemical destruction of HD by H_3^+ is dominant, the proportionality to ζ is no more fulfilled since the abundance of H_3^+ is itself proportional to the cosmic ray ionization rate.

This point is illustrated in Fig. 6 where we display the column densities of HD and OH divided by ζ, computed for models of constant density (n_H = 500 $\mathrm{cm^{-3}}$) and different values of ζ as a function of the visual extinction. The ratios are independent of ζ in a range of A_V between 0.001 and 0.1 for HD and 0.001 and 1 for OH.

3.2.2. Dependence on the density and radiation field

D/HD transition

Figure 7 displays the normalized abundances of D and HD calculated in models with densities between 100 and 10^5 $\mathrm{cm^{-3}}$ and $\chi = 1$. The respective atomic and molecular abundances of deuterium at the edge of the cloud are directly obtained from the balance between photodissociation and formation on dust.

$$\left.\frac{n(\mathrm{HD})}{n(\mathrm{D})}\right|_{\mathrm{edge}} = \frac{\mathcal{FR}(\mathrm{HD})}{\mathcal{P}_0(\mathrm{HD})} = \frac{6.3 \times 10^{-17} n_\mathrm{H}}{2.6 \times 10^{-11}} = 2.4 \times 10^{-6}\, n_\mathrm{H}$$

Table 6. Reaction rate coefficients.

Reactions						Reference
D^+	H_2	$\longrightarrow$	H^+	HD		(a)
		k_1	2×10^{-9}			
H^+	HD	$\longrightarrow$	D^+	H_2		(a)
		k_1'	$1 \times 10^{-9} e^{-464/T}$			
D	H_2	$\longrightarrow$	H	HD		(b)
		k_2	$7.5 \times 10^{-11} e^{-3820/T}$			
HD	H	$\longrightarrow$	H_2	HD		(b)
		k_2'	$7.5 \times 10^{-11} e^{-4240/T}$			
H^+	D	$\longrightarrow$	D^+	H		(c)
		k_3	$1.0 \times 10^{-9} e^{-41/T}$			
D^+	H	$\longrightarrow$	H^+	D		(c)
		k_3'	1×10^{-9}			
He^+	H_2	$\longrightarrow$	H	H^+	He	(d)
		k_4	$1.1 \times 10^{-13} (T/300)^{-0.24}$			
H^+	O	$\longrightarrow$	O^+	H		(e)
		k_5	$6 \times 10^{-10} e^{-227/T}$			
C^+	OH	$\longrightarrow$	CO^+	H		(f)
		k_6	7.7×10^{-10}			

Reactions						Reference
H	cr	$\longrightarrow$	H^+	e^-		(f)
		k_ζ	$0.46 \times \zeta$			
He	cr	$\longrightarrow$	He^+	e^-		(f)
		k_ζ'	$0.5 \times \zeta$			
H_2	cr	$\longrightarrow$	H^+	H	e^-	(g)
		k_ζ''	$0.04 \times \zeta$			
H_2	$h\nu$	$\longrightarrow$	H	H		(h)
		$\mathcal{P}_0(H_2)$	3.2×10^{-11}			
HD	$h\nu$	$\longrightarrow$	H	D		(h)
		$\mathcal{P}_0(HD)$	2.6×10^{-11}			
C	$h\nu$	$\longrightarrow$	C^+	e^-		(h)
		$\mathcal{P}_0(C)$	$1.7 \times 10^{-10} \cdot \exp(-2.96 A_V)$			
H^+	e^-	$\longrightarrow$	H	$h\nu$		(f)
		$\alpha(H^+)$	$3.5 \times 10^{-12} (T/300)^{-0.70}$			
He^+	e^-	$\longrightarrow$	He	$h\nu$		(f)
		$\alpha(He^+)$	$4.5 \times 10^{-12} (T/300)^{-0.67}$			
H_3O^+	e^-	$\longrightarrow$	H_2O	H	α_1	(i)
			OH	H_2	α_2	
			OH	H	H α_3	
		α_1	$1.1 \times 10^{-7} (T/300)^{-0.65}$			
		α_2	$5.8 \times 10^{-8} (T/300)^{-0.65}$			
		α_3	$1.5 \times 10^{-7} (T/300)^{-0.65}$			

All rates are in $cm^3\ s^{-1}$ excepted those of photodissociation, photoionization and ionization by cosmic rays wich are in s^{-1}. *References:* (a) Smith, D., Adams, N. G., & Alge, E. 1982, ApJ, 263, 123. (b) Stancil, P. C., Lepp, S., & Dalgarno, A. 1998, ApJ, 509, 1. (c) Watson, W. D. 1976, Rev. Mod. Phys., 48, 513. (d) Böringer, H., & Arnold, F. 1986, J. Chem. Phys., 84, 1459. (e) Federer, W., et al. 1984, Phys. Rev. Lett., 52, 2084. (f) Prasad, S. S., & Huntress, W. T. 1980, ApJS, 43, 1. (g) Private communication from Alex Dalgarno. (h) Obtained from our numerical model computing the photodissociation of the chemical species. (i) Vejby-Chriestensen, J., et al. 1997, ApJ, 483, 531.

where $\mathcal{P}_0$(HD) is the photodissociation rate of HD in s^{-1} at the edge of the cloud.

We introduce $A_{V_{\rm D/HD}}$, the value of the visual extinction where $n(D) = n(HD) = \xi_D \cdot n_H/2$ with ξ_D, the elemental abundance of deuterium relative to H.

In the case where HD is formed by $D^+ + H_2$, neglecting the contribution of atomic hydrogen and assuming that C is the main source of electrons, we obtain a relation between the photodissociation rate at the D/HD transition, the different rate coefficients, and the elemental abundances relative to H of He (ξ_{He}), C (ξ_C) and O (ξ_O).

$$P_\tau(\mathrm{HD})|_{\rm transition} = \frac{k_3[k_\zeta' \xi_{He} + k_\zeta''/2]}{[\alpha(H^+)\xi_C + k_5 \xi_O]}. \quad (20)$$

The photodissociation rate (in s^{-1}) at the optical depth τ can be expressed as:

$$\mathcal{P}_\tau(\mathrm{HD}) = \chi \mathcal{P}_0(\mathrm{HD}) f(N(\mathrm{HD})) e^{-\beta A_V} \quad (s^{-1}) \quad (21)$$

where $\exp(-\beta A_V)$ corresponds to the continuum absorption by grains and $f(N(HD))$ represents the self-shielding function and depends only on N(HD). We ignore the possible overlap with H_2 lines which is a complex function of the column density of H_2.

The substitution of this expression in Eq. (20) implies at first sight that $A_{V_{\rm D/HD}}$ should not depend on the density. This first guess should be tempered since the thermal profile is density dependent and $A_{V_{\rm D/HD}}$ is a sensitive function of the kinetic temperature via the rate coefficients. This can be seen in Fig. 8

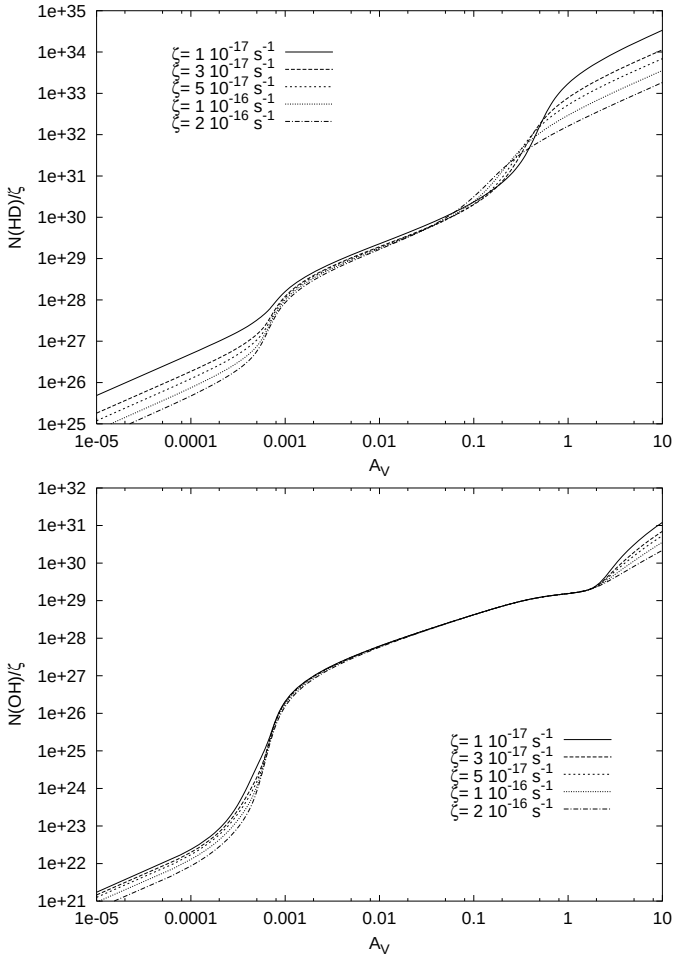

Fig. 6. N(HD)/ζ and N(OH)/ζ in function of the visual extinction for a model of density $n_{\rm H}$ = 500 cm^{-3} and χ = 1, in a log-log diagram.

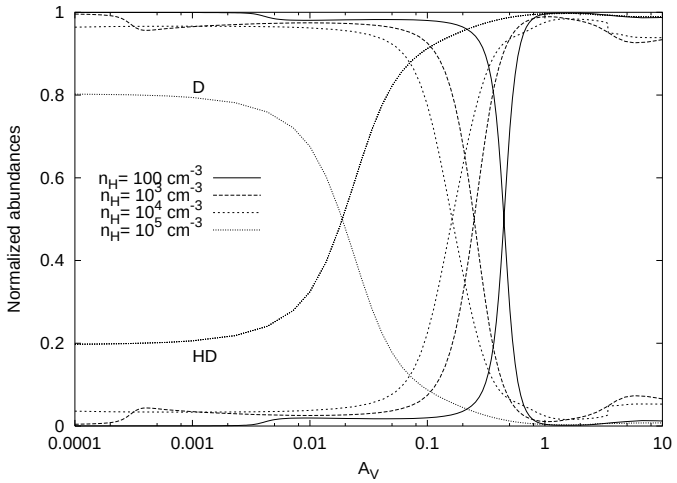

Fig. 7. D/HD transition for models with densities between 100 and 10^5 cm^{-3} and χ = 1.

which displays $A_{V_{\rm D/HD}}$ as well as the temperature at the D/HD transition, $T_{\rm D/HD}$, for different densities and for χ = 1. This behaviour is different from the H/H$_2$ transition where the formation rate on dust is proportional to the square of the density. The dependence of $A_{V_{\rm D/HD}}$ on χ is ln(χ).

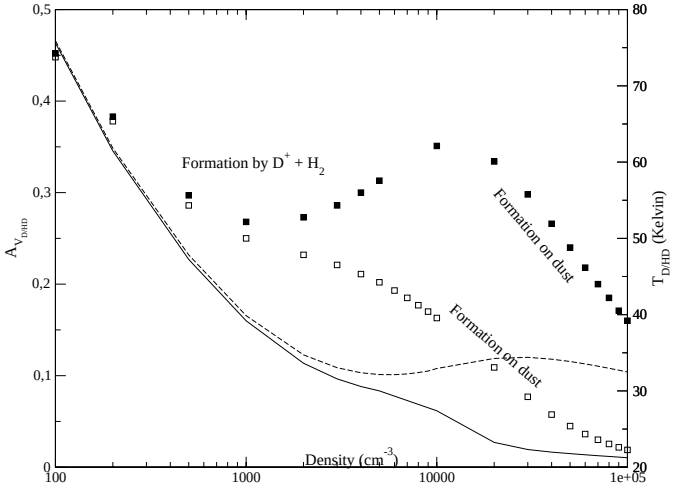

Fig. 8. Position of the transition D/HD, $A_{V_{\rm D/HD}}$ (squares) and temperature of the gas (lines) at the transition as a function of the density. Blank squares and dashed line correspond to the standard formation rate of HD on dust ($\mathcal{FR}$(HD) = 6.3×10^{-17} × $n_{\rm H}$). Black squares and full line correspond to $\mathcal{FR}$(HD) = 6.3×10^{-18} × $n_{\rm H}$. For all models, χ = 1.

As described in Sect. 2.3, at densities higher than 5000 cm^{-3}, the formation of HD occurs principally on dust. In this case, at the D/HD transition:

$$P_\tau({\rm HD})|_{\rm transition} = k_{\rm ads} = 6.3 \times 10^{-17} n_{\rm H}. \quad (22)$$

With the photodissociation rate expression (Eq. (21)), we derive that $A_{V_{\rm D/HD}}$ is now a function of ln($\chi/n_{\rm H}$). This logarithmic behaviour can be seen in Fig. 8 for densities higher than 5000 cm^{-3} when standard formation rate of HD on dust is assumed.

Dependence on the formation rate of HD on dust

The formation rate of HD on dust is not well known. We discuss the significance of the mechanism introducing a formation rate with a sticking factor 10 times less than the standard hypothesis. Considering the full squares symbols in Fig. 8 two different regimes are still found for $A_{V_{\rm D/HD}}$.

As expected, the regime corresponding to formation on dust is taking place at larger densities ($n_{\rm H} \geq 20000$ cm^{-3}) than with the standard rate.

We have compared the computed column densities of HD at a visual extinction of 1, obtained using the two different HD formation rates on dust. The differences in the column densities are smaller than 10% for densities between 10^3 and 10^4 cm^{-3} and of the order of 30 % for higher densities.

Dependence on the intensity of the incident radiation field

Figure 9 displays $A_{V_{\rm D/HD}}$ and the temperature at the transition as a function of the scaling factor χ of the ISRF for models with densities 500 and 10^5 cm^{-3}. When $n_{\rm H}$ = 500 cm^{-3}, the formation of HD occurs always through the gas phase reaction between D$^+$ and H$_2$ and the variation of $A_{V_{\rm D/HD}}$ with χ is almost logarithmic as predicted by Eq. (20). For $n_{\rm H} = 10^5$ cm^{-3} and χ lower than 2600 the formation of HD occurs on dust. For larger

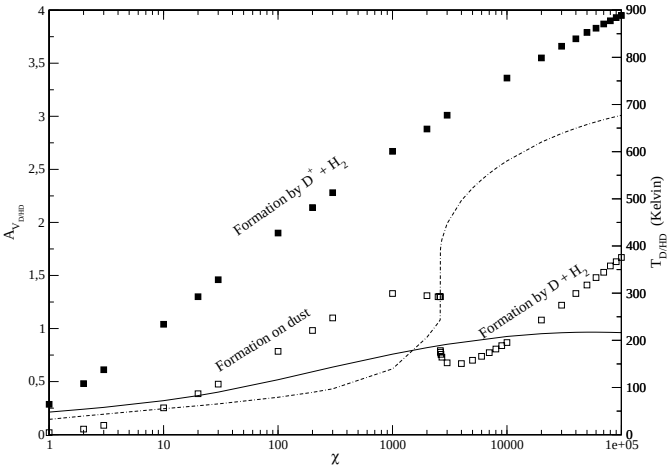

Fig. 9. Position of the transition D/HD, $A_{V_{\rm D/HD}}$ (squares) and temperature (lines) at the transition versus χ. Black squares and full line correspond to models of density 500 cm^{-3} while blank squares and dashed line correspond to models of density 10^5 cm^{-3}.

values of χ, the temperature may reach several hundred Kelvin allowing the neutral-neutral reaction D + H_2 to become dominant. The high efficiency of this process moves the position of the transition D/HD closer to the edge of the cloud, producing a discontinuity as shown on the figure. Under these conditions, $A_{V_{\rm D/HD}}$ is given by:

$$\mathcal{P}_\tau(\mathrm{HD}) + k_2' n(\mathrm{H}) = k_2 n(\mathrm{H_2}) \simeq \frac{k_2}{2} n_{\rm H} \qquad (23)$$

where the reverse reaction may not be negligible. Once more, a logarithmic dependence on χ as $\ln(\chi/n_{\rm H})$ is obtained for $A_{V_{\rm D/HD}}$, as displayed in the figure.

3.3. Validity of the equilibrium model

Our model is steady state. A characteristic timescale can be derived from the destruction processes of HD.

$$t(\mathrm{HD})_{\rm dest.} = \frac{n(\mathrm{HD})}{\text{destruction rate in cm}^{-3}\ \text{s}^{-1}}.$$

While photodissociation is the main process of destruction of HD, the characteristic timescale is equal to the inverse of the photodissociation rate (in s^{-1}). Its value is $1000/\chi$ years at the edge of the cloud and it increases when self-shielding and dust absorption become significant. In the absence of photoprocesses, HD is principally destroyed by H_3^+, via reaction 14. As H_3^+ is directly formed via the reaction between H_2^+ and H_2 and destroyed by reactions with O, CO and dissociative recombination, the chemical time associated to HD is inversely proportional to n_H. As long as this chemical timescale is smaller than a dynamic time scale, for example the free fall time, the steady state approximation is adequate. This condition is reasonably fulfilled in the translucent part of the model. Time dependent models such as those presented by Lee et al. (1996) for H_2 and CO may be more appropriate in the more obscured regions.

4. Comparison with observations

4.1. UV absorption of HD

The present model enables interpretation of the available and forthcoming observations of UV absorption transitions of H, D, H_2, HD, and other species towards diffuse and translucent clouds. At present, the high sensitivity of FUSE allows to extend the sample of diffuse clouds in front of bright stars obtained by Copernicus and IUE satellites towards lines of sight involving more reddened stars. However, derivation of the column density of HD is subject to large uncertainties since HD lines are partially saturated and several components may be present on the lines of sight. We have shown in Sect. 3.1, that the elemental deuterium to hydrogen ratio is not simply given by N(HD)/2N(H_2). Table 7 displays N(D)/N(H) and N(HD)/2N(H_2) for different values of the molecular fraction deduced from our standard model ($n_{\rm H}$ = 500 cm^{-3}, χ = 1). Results are given for elemental D/H ratios of 1×10^{-5} and of 2×10^{-5}. The values of both N(D)/N(H) and N(HD)/2N(H_2) are proportional to the elemental ratio $\xi_{\rm D}$. As expected they bracket the actual value of $\xi_{\rm D}$.

For high z objects, UV absorption transitions are shifted to the visible. The first detection of HD (N(HD) = 1–4$\times10^{14}$ cm^{-2}) in front of a quasar (PKS 1232+082) is reported by Varshalovich et al. (2001). On the other hand, Petitjean et al. (2000) find a column density of H_2 of 6×10^{16} cm^{-2} and a molecular fraction of 1.5×10^{-4} towards the same line of sight. We can deduce from these values N(HD)/2N(H2) of 8.3×10^{-4} – 3.3×10^{-3}. This surprising result may come from the specific physical conditions present in extragalactic environment.

4.2. Infrared intensities of HD rotational transitions

Our model of the HD excitation allows to derive the intensities of the pure rotational transitions of HD. As the transitions probabilities are low, the intensities $I_{J,J-1}$ are directly obtained from an optically thin approximation:

$$I_{J,J-1} = \frac{N(J)}{4\pi} A_{J,J-1} E_{J,J-1}$$

where $N(J)$ is the column density of the upper level of the transition, $A_{J,J-1}$, the Einstein emission probabilities and $E_{J,J-1}$ the energy of the transition. We display the corresponding values in Tables 8 and 9 for the transitions at 112 μm ($J = 1 \rightarrow 0$) and 56 μm ($J = 2 \rightarrow 1$). Results are expressed in erg s^{-1}cm^{-2}sr^{-1} and have been calculated for a total visual extinction of 10 magnitudes and densities between 100 and 10^5 cm^{-3} and χ between 1 and 10^5. The kinetic temperature at the emission maximum of the transition and the corresponding visual extinction are also displayed in Tables 8 and 9 for each model in order to better explain the intensity values. The models sample a large range of physical conditions.

The magnitudes of the intensities of both infrared transitions are principally driven by the magnitude of the radiation field. The position of the local emissivity maximum is shifted towards larger values of the visual extinction as χ increases and the temperature increases as well. The two transitions are not

Table 7. Column densities ratios in function of f.

f	N(D)/N(H)$^{(a)}$	N(HD)/(2×N(H_2))$^{(a)}$
0.1	2.2(−5)	3.0(−6)
	1.1(−5)	1.5(−6)
0.2	2.5(−5)	2.0(−6)
	1.2(−5)	1.1(−6)
0.3	2.8(−5)	1.6(−6)
	1.4(−5)	7.8(−7)
0.4	3.2(−5)	1.3(−6)
	1.6(−5)	6.7(−7)
0.5	4.1(−5)	1.0(−6)
	2.0(−5)	5.1(−7)
0.6	5.0(−5)	8.2(−7)
	2.4(−5)	4.0(−7)
0.7	6.7(−5)	6.7(−7)
	3.3(−5)	3.4(−7)
0.8	9.6(−5)	5.5(−7)
	4.8(−5)	2.8(−7)
0.9	2.0(−4)	6.7(−7)
	1.0(−4)	3.2(−7)
0.99	2.7(−4)	1.9(−5)
	1.4(−4)	9.3(−6)

(a) Values have been obtained in the case of the standard model ($n_{\rm H}$ = 500 cm^{-3}, χ = 1). For each value of f (molecular fraction), the first line corresponds to $\xi_{\rm D}$ = 2×10^{-5} and the second one to $\xi_{\rm D}$ = 1×10^{-5}. Numbers in parentheses refer to power of ten.

Table 8. Intensities at 112 μm.

	$n_{\rm H}$ (cm^{-3})				
	100	1000	1×10^4	1×10^5	1×10^6
χ					
1	2.5(−8)	2.3(−8)	2.3(−8)	1.2(−8)	2.2(−9)
	78	40	104	143	155
	0.45	0.26	1.8(−5)	6.3(−7)	1.0(−7)
10	7.7(−8)	1.1(−7)	2.1(−7)	2.5(−7)	1.7(−7)
	111	59	47	50	46
	1.3	1	0.78	0.35	0.07
100	1.9(−7)	4.4(−7)	7.8(−7)	8.6(−7)	8.7(−7)
	145	97	76	70	69
	2	1.9	1.5	1	0.45
10^3	3.7(−7)	1.2(−6)	2.0(−6)	2.2(−6)	2.6(−6)
	176	156	124	108	111
	2.8	2.8	2.35	1.7	1.0
10^4	5.6(−7)	2.1(−6)	4.2(−6)	4.7(−6)	4.9(−6)
	190	207	208	157	151
	3.6	3.6	3.1	2.7	2.1
10^5	7.0(−7)	3.1(−6)	5.9(−6)	5.7(−6)	6.4(−6)
	189	238	248	165	154
	4.8	4.4	4.3	4.1	3.5

For each couple of density and χ, the first line gives the intensity of the transition calculated for A_V = 10 in erg s^{-1} cm^{-2} sr^{-1}. The second and third lines give the temperature and the visual extinction corresponding to the local emissivity maximum. Numbers in parentheses refer to power of ten.

exactly peaking at the same visual extinctions since the 56 μm transition corresponds to a higher excitation. The intensity of the 112 μm transition reported by Wright et al. (1999) towards the Orion Bar is (8.7 ± 1.5) × 10^{-6} erg s^{-1} cm^{-2} sr^{-1}. As the radiation field in this environment is estimated to be close to 4.4×10^4 times the ISRF (Parmar et al. 1991; Hogerheijde et al. 1995) and the mean density value is 2.5×10^5 cm^{-3} (Jansen et al. 1995), the observed value is compatible with our results. However, the knowledge of the actual geometry is critical to make quantitative predictions. The ratio of the emissivities of the 112 μm and 56 μm transitions is a very sensitive function of both n_H and χ. However, the 56 μm has a lower intensity except for very high density and very large radiation field conditions. It has not been detected with ISO. The future HERSCHEL mission will allow to search for the 112 μm transition at a much higher sensitivity than ISO with the PACS instrument. A sensitivity of some 10^{-14} erg s^{-1} cm^{-2} in a field of view of 47″ × 47″ is expected. The 56 μm transition is unfortunately beyond the reserved wavelength range of HERSCHEL.

5. Conclusion and perspectives

We have presented PDR models where chemistry and rotational excitation of HD is explicitly introduced with the most recent molecular data. Thermal balance is solved in parallel to chemical equilibrium. As for H_2, photodissociation in the discrete UV transitions of Lyman and Werner electronic bands controls the atomic to molecular deuterium transition. However, contrary to H_2, gas phase chemical formation of HD is occurring via the $D^+ + H_2$ reaction in low and medium density clouds. Competing formation mechanisms of HD are taking place for high density conditions. Formation on dust may be preponderant in cold dense regions whereas the neutral-neutral reaction between D and H2 takes place under high interstellar radiation field conditions where the temperature may reach several hundred Kelvin at the edge of the cloud. The D/HD transition occurs for larger visual extinctions than for H/H_2 since self-shielding effects are much less efficient due to the small elemental abundance of deuterium. We have also given the critical densities for different temperatures: at low densities ($n_{\rm H} \leq$ 1000 cm^{-3}), the excitation of the level J = 1 of HD is sub-thermal whether the medium is atomic or molecular. The critical density values increase significantly when J increases. This remains true for vibrational energy levels for which the Einstein emission coefficients are several 10^{-5} s^{-1} and the vibrational de-excitation coefficients are of the order of 10^{-15} at maximum.

Table 9. Intensities at 56 μm.

	n_H (cm^{-3})				
	100	1000	1×10^4	1×10^5	1×10^6
χ					
1	2.9(−10)	7.0(−11)	1.0(−10)	6.1(−11)	7.2(−12)
	87	45	111	142	161
	0.35	0.14	1.2(−5)	6.3(−7)	6.8(−8)
10	2.4(−9)	1.8(−9)	8.5(−9)	2.3(−8)	7.6(−9)
	122	65	51	54	52
	1.1	0.9	0.6	0.28	0.025
100	1.2(−8)	3.5(−8)	1.8(−7)	3.3(−7)	3.3(−7)
	152	109	84	75	75
	1.9	1.8	1.4	0.9	0.36
10^3	3.2(−8)	2.9(−7)	1.7(−6)	3.7(−6)	6.3(−6)
	181	168	142	128	143
	2.7	2.6	2.1	1.4	0.74
10^4	5.6(−8)	8.9(−7)	1.2(−5)	2.7(−5)	2.4(−5)
	190	215	272	390	404
	3.6	3.4	2.6	1.6	1.2
10^5	6.7(−8)	1.6(−6)	2.5(−5)	3.9(−5)	3.4(−5)
	189	242	378	439	402
	4.8	4.2	3.0	2.8	2.5

For each couple of density and χ, the first line gives the intensity of the transition calculated for $A_V = 10$ in erg s^{-1} cm^{-2} sr^{-1}. The second and third lines give the temperature and the visual extinction corresponding to the local emissivity maximum. Numbers in parentheses refer to power of ten.

We have derived the main properties of the atomic to molecular deuterium transition for different densities and enhancement factors of the ISRF. The sensitivity of the results to the cosmic ray ionization rate, the formation rate on dust and the elemental deuterium abundance are studied. We extend the previous analytical expressions of the steady state abundance of HD in the case where H_2 is prevailing but when photoprocesses are still dominant for HD.

The present model is valuable to interpret the observations of H_2 and HD in a variety of physical conditions. We have shown that $N(\mathrm{HD})/2N(H_2)$ is a lower limit to the elemental deuterium abundance in diffuse and translucent clouds whereas $N(\mathrm{D})/N(\mathrm{H})$ leads to an upper limit. So, the recent detections of HD with FUSE should be analyzed with care. The intensities of the pure rotational transitions are predicted for a large range of density and enhancement factors of the ISRF. The values are compatible with the detection of the 112 μm transition in the Orion Bar by Wright et al. (1999). It is also shown that the intensity of the 56 μm transition is below that of the 112 μm transition for density below 10^5 cm^{-3} and $\chi \leq 10^5$. Up to now, this transition has not been detected by ISO. The future HERSCHEL mission will allow to search for HD 112 μm at a higher sensitivity. A natural extension of our model is to include the vibrational excitation of HD. Detection of the 1–0 R(5) transition of HD at 2.46 μm by Ramsay Howat et al. (2002) is interpreted as a result of chemical excitation. This could be tested in such models. However the fast vibrational radiative decay of HD of several 10^{-5} s^{-1} implies critical densities at least of the order of 10^{10} cm^{-3} and the vibrational level populations will be sub-thermal in most cases. It is therefore not surprising that vibrationally excited HD has not been detected in the Hubble Space Telescope (HST) spectra towards HD39603, a PDR region of density of several 10^4 cm^{-3} in the NGC2023 nebula whereas a rich spectrum of vibrationnally excited hydrogen has been obtained by Meyer et al. (2001).

Future efforts will also be put on MHD shock models following the treatments developed for H_2 (Wilgenbus et al. 2000). The detection of the 0–0 R(5) transition of HD at 19.43 μm by Bertoldi et al (1999) in the OMC1 cloud is due to shock excitation.

Acknowledgements. We thanks Thomas Nodé Langlois who contributed at an early stage to the implementation of HD to the PDR model. We thanks also the referee for his thoughtful remarks which improved the manuscript considerably. Support from the Programme National du Milieu Interstellaire (PCMI) is gratefully acknowledged.

References

Abgrall, H., Roueff, E., & Viala, Y. P. 1982, A&AS, 50, 505
Abgrall, H., Le Bourlot, J., Pineau des Forêts, G., et al. 1992, A&A, 253, 525
Abgrall, H., Roueff, E., & Drira, I. 2000, A&AS, 50, 505
Abgrall, H., & Roueff, E. 2002, in preparation
Allison, & Dalgarno, A. 1970, Atom. Data, 1, 289
Bakes, E. L. O., & Tielens, A. G. G. M. 1994, ApJ, 427, 822
Bertoldi, F., Timmermann, R., Rosenthal, D., Drapatz, S., & Wright, C. 1999, A&A, 346, 267
Black, J. H., & Dalgarno, A. 1973, ApJ, 185, L101
Black, J. H., & Dalgarno, A. 1976, ApJ, 203, 132
Bluhm, H., & de Boer, K. S. 2002, A&A, 379, 82
Bohlin, R. C., Savage, D., & Drake, J. F. 1978, ApJ, 224, 132
Boissé, P., Le Petit, F., Pineau des Forêts, G., & Roueff, E. 2002, A&A, submitted
Draine, B. 1978, ApJS, 36, 595
Federman, S. R., Glassgold, A., & Kwan 1979, ApJ, 227, 466
Federman, S. R., Weber, J., & Lambert, D. L. 1996, ApJ, 463, 181
Ferlet, R., André, M., Hébrard, G., et al. 2000, ApJ, 538, L69
Fitzpartrick, E. L., & Massa, D. 1990, ApJS, 72, 163
Flower, D. R., & Roueff, E. 1999, MNRAS, 309, 833
Flower, D. R., Le Bourlot, J., Pineau des Forêts, G., & Roueff, E. 2000, in H_2 in space, ed. Combes and Pineau des Forêts (Cambridge University Press), 23
Galli, D., & Palla, F. 1998, A&A, 335, 403
Gerlich, D., Herbst, E., & Roueff, E. 2002, submited to PSS.
Gry, C., Boulanger, F., Nehmé, C., et al. 2002, A&A, in press
Hartquist, T. W., Black, J. H., & Dalgarno, A. 1978, MNRAS, 185, 643
Hogerheijde, M. R., Jansen, D. J., & van Dishoeck, E. F. 1995, A&A, 294, 792
Hollenbach, D. J., & Mac Kee, C. F. 1979, ApJ, 41, 555

Hollenbach, D. J., & Tielens, A. G. G. M. 1999, Rev. Mod. Phys., 71, 173
Jansen, D. J., Spaans, M., Hogerheijde, M. R, & van Dishoeck, E. F. 1995, A&A, 303, 541
Jura, M. 1975, ApJ, 197, 581
Lacour, S., Sonnentrucker, P., Ferlet, R., et al. 2001, AAS, 199.6510
Le Bourlot, J., Roueff, E., & Viala, Y. 1987, A&A, 188, 137
Le Bourlot, J., Pineau des Forêts, G., Roueff, E., & Flower, D. 1993, A&A, 267, 233
Le Bourlot, J., Pineau des Forêts, G., Roueff, E., Dalgarno, A., & Gredel, R. 1995, ApJ, 449, 178
Le Bourlot, J. 2000, A&A, 360, 656
Lee, H. H., Herbst, E., Pineau des Forets, G., Roueff, E., & Le Bourlot, J. 1996, A&A, 311, 390
Lemoine, M., et al. 1999, New Astron., 4, 231
Le Petit, F., & Roueff, E. 2002, in The Dissociative Recombination of Molecules with Electrons, ed. S. Guberman (Kluwer Academic, Plenum Publisher), to be published
Linsky, J. L., Diplas, A., Wood, B. E., et al. 1995, ApJ, 541, 335
Lis, D., Roueff, E., Gerin, M., et al. 2002, ApJ, 571, L55
Loinard, L., Castets, A., Ceccarelli, C., et al., A&A, 357, 1169
Mathis, J. S., Rumpl, W., & Nordsieck, K. H. 1977, ApJ, 217, 425
Meyer, D. M., Cardelli, J. A., & Sofia, U. J. 1997, ApJ, 490, L103
Meyer, D. M., Jura, M., & Cardelli, J. A. 1998, ApJ, 493, 222
Meyer, D. M., Lauroesch, J. T., Sofia, U. J., & Bertoldi, F. 2001, ApJ, 553, L59
Parmar, P. S., Lacy, J. H., & Achtermann, J. M. 1991, ApJ, 372, L25
Petitjean, P., Srianand, R., & Ledoux, C 2000, A&A, 364, L26
Pineau des Forêts, G., Roueff, E., & Flower, D. R. 1989, MNRAS, 240, 167
Rachford, B., et al. 2001, ApJ, 555, 839
Ramsay Howat, S. K., Timmermann, R., Geballe, T. R., Bertoldi, F., & Mountain, C. M. 2002, ApJ, 566, 905
Roberts, H., & Millar, T. J. 2000, A&A, 361, 388
Roberts, H., & Millar, T. J. 2000, A&A, 364, 780
Roueff, E., & Zeippen, C. J. 1999, A&A, 343, 1005
Roueff, E., & Zeippen, C. J. 2000, A&AS, 142, 475
Roueff, E., Tiné, S., Pineau des Forêts, G., Falgarone, E., & Gerin, M. 2000, A&A, 354, L63
Roueff, E. 2002, in proceedings of the XIII IAP Coll.
Stancil, P. C., Lepp, S., & Dalgarno, A. 1998, ApJ, 509, 1
Savage, B. D., & Sembach, K. R. 1996, Ann. Rev. Astro. Astrophys., 34, 279
van der Tak, F. F. S., Schilke, P., Müller, H. S. P. 2002, A&A, 388, L53
van Dishoeck, E. F., & Black, J. H. 1986, ApJS, 62, 109
van Dishoeck, E. F., & Black, J. H. 1988, ApJ, 334, 771
Varshalovich, D. A., Ivanchik, A. V., Petitjean, P., Srianand, R., & Ledoux, C. L. 2001, AL, 27, 683
Viala, Y., Roueff, E., & Abgrall, H. 1988a, A&A, 190, 215
Viala, Y., Letzelter, C., Eidelsberg, M., & Rostas, F. 1988b, A&A, 193, 263
Wilgenbus, D., Cabrit, S., Pineau des Forêts, G., & Flower, D. 2000, A&A, 356, 1010
Wright, C. M., van Dishoeck, E. F., Cox, P., & Kessler, M. F. 1999, ApJ, 515, L29